Published in final edited form as:
Curr Opin Colloid Interface Sci. 2011 June ; 16(3): 215–227. doi:10.1016/j.cocis.2011.01.008.

Targeted Nanocarriers for Imaging and Therapy of Vascular Inflammation

Ann-Marie Chacko, **Elizabeth D. Hood**, **Blaine J. Zern**, and **Vladimir R. Muzykantov***
Department of Pharmacology and Institute for Translational Medicine and Therapeutics, University of Pennsylvania, School of Medicine, Philadelphia, PA 19104, USA

Abstract

Vascular inflammation is a common, complex mechanism involved in pathogenesis of a plethora of disease conditions including ischemia-reperfusion, atherosclerosis, restenosis and stroke. Specific targeting of imaging probes and drugs to endothelial cells in inflammation sites holds promise to improve management of these conditions. Nanocarriers of diverse compositions and geometries, targeted with ligands to endothelial adhesion molecules exposed in inflammation foci are devised for this goal. Imaging modalities that employ these nanoparticle probes include radioisotope imaging, MRI and ultrasound that are translatable from animal to human studies, as well as optical imaging modalities that at the present time are more confined to animal studies. Therapeutic cargoes for these drug delivery systems include diverse anti-inflammatory agents, anti-proliferative drugs for prevention of restenosis, and antioxidants. This article reviews recent advances in the area of image-guided translation of targeted nanocarrier diagnostics and therapeutics in nanomedicine.

Keywords

Nanoparticles; Drug delivery; Molecular imaging; Cell adhesion molecule; Inflammation; Nanomedicine

1. Introduction

The endothelium, a cellular monolayer lining the inner surface of blood vessels, is an important therapeutic target for a variety of vascular inflammatory diseases including atherosclerosis, ischemia-reperfusion injury, stroke, and hypertension. The non-invasive, real-time imaging of molecular and functional changes in the endothelium at early stages in vascular pathologies will help to identify diseased tissue, enhance and refine differential diagnoses via identification of specific molecular markers, and guide individualized therapies and disease monitoring. Molecular imaging can also play an important role in studying the delivery and effects of novel therapeutics targeted to the vascular endothelium. This latter goal, namely achieving high levels of control of spatiotemporal parameters of

***To whom correspondence should be addressed:** Vladimir Muzykantov, MD, PhD Professor of Pharmacology and Medicine Chair, Graduate Group in Pharmacological Sciences Director, Program in Targeted Therapeutics, ITMAT Sr.Investigator, Institute for Environmental Medicine University of Pennsylvania School of Medicine 1 John Morgan Building, 3620 Hamilton Walk Philadelphia, PA 19104-6068 Tel: (215) 898-9823; Fax: (215)-898-0868 muzykant@mail.med.upenn.edu.

molecular interventions in endothelial components of vascular pathology, represent an enormous challenge, yet holds the promise of improving management of many vascular, pulmonary, cerebral, oncologic, and metabolic diseases [1–3].

2. Molecular markers of pathological endothelial activation

Vascular inflammation represents a cascade of events including the endothelial expression of molecular determinants involved in recruitment of leukocytes, which propagate the inflammatory process and, in many cases, may aggravate tissue injury (Figure 1A). However, using endothelial molecules selectively exposed in sites of inflammation enables targeting of diagnostic and therapeutic nanocarriers to pathologically activated vascular endothelium (Figure 1B) [4]. In particular, endothelial cell adhesion molecules (CAMs) are markers of inflammation that promote leukocyte adhesion to activated vascular endothelium (Table 1). P- and E-selectins are normally absent on the endothelial surface and get exposed at early stages of the inflammatory cascade. Selectins bind sialylated, fucosylated, and sulfated carbohydrate ligands (e.g. sialyl-Lewis X (sLe^x) on circulating leukocytes and thus mediate their tethering and rolling. Vascular cell adhesion molecule-1 (VCAM-1) and intercellular adhesion molecule-1 (ICAM-1) are transmembrane proteins supporting the firm endothelial adhesion of leukocytes through their β1 and β2 integrins [5]. VCAM-1, like selectins, is normally absent on the quiescent endothelium, while ICAM-1 is constitutively expressed on endothelial surface, yet its expression is up-regulated several fold in sites of inflammation [6]. Thus selectins and VCAM-1 can be used for detection of inflammation, whereas ICAM-1 can be used both for prophylactic and relatively selective therapeutic drug delivery [4]. In addition to these inducible adhesion molecules, platelet-endothelial adhesion molecule-1 (PECAM-1) is constitutively present on the order of millions of copies on the endothelium surface. It is unlikely that PECAM-1 could be used for selective delivery of imaging probes and drugs to inflammatory foci, but it serves as an attractive target for pan-endothelial prophylactic interventions [7].

This review focuses on the exploration of CAMs as targets for detection and treatment of vascular inflammation. We will give an overview of molecular imaging techniques, and describe nanocarrier platforms for targeting imaging agents and therapeutics. Finally, we will further highlight animal studies exploring CAM-targeted nanoparticles for site-specific diagnostic imaging and for therapeutic interventions in vascular inflammatory diseases and other disorders associated with pathological endothelial activation.

3. Molecular imaging modalities

A targeted molecular imaging nanoparticle probe, consists of: (1) a label or probe (e.g. radionuclide, iron oxide, gadolinium-chelate, gas- or liquid-filled bubble, fluorophore, etc. or any combination thereof) stably bound to carrier, (2) a ligand that directs the nanoparticle to the molecular target (e.g. monoclonal antibody (Ab), Ab fragment, peptide, small molecule), and (3) a carrier or nanoparticle coupling these components to a single entity (Figure 2). Depending on the requirements of longevity in circulation and intracellular delivery of the probe, a nanocarrier may also contain masking (e.g. polyethylene glycol (PEG)) and membrane-permeating moieties, respectively. Optimal imaging of vascular inflammation can be achieved with nanoparticle probes whose pharmacokinetics favors delivery and specific binding to the target, and fast blood clearance.

Modalities for detection of imaging probes differ in spatial and temporal resolution, depth of signal penetration, detection threshold of imaging probes, and the availability of imaging probes (Table 2). This section will briefly introduce the features of modalities available for tracing nanoparticle imaging probes *in vivo* and have the most potential for clinical translation as probes become available.

3.1 Nuclear imaging: PET and SPECT

Positron emission tomography (PET) and single photon emission computed tomography (SPECT) are noninvasive 3-D tomographic imaging techniques that detect gamma (γ-rays emitted from radionuclide-labeled probes deep within living tissue, capable of detecting radiotracers in nanomolar to picomolar (10^{-9} M to 10^{-} M) concentration levels with fast temporal resolution in real time [8]. PET is designed to indirectly detect positron (β^{+})-emitting isotopes that emit β^{+} particles, which encounter electrons in the tissue. The consequent annihilation produces two coincident 511-keV photons that are detected by the PET detector system. PET isotopes include fluorine-18 (^{18}F, half-life ($t_{½}$) = 110 min), copper-64 (^{64}Cu, $t_{½}$ = 12.2 h), and iodine-124 (^{124}I, $t_{½}$ = 4.2 d). SPECT detects single low energy -rays directly emitted from the decay of specific radioisotopes including technetium-99m (^{99m}Tc, $t_{½}$ = 6 h), iodine-123 (^{123}I, $t_{½}$ = 13.2 h), and indium-111 (^{111}In, $t_{½}$ = 2.8 d). Planar -scintigraphy is another commonly used method to observe the distribution of direct γ-emitting isotopes. However, unlike SPECT, it produces 2-D images inadequate for quantitatively measuring tracer distribution. PET has higher sensitivity and temporal resolution relative to SPECT and MRI. PET has slightly higher spatial resolution than SPECT, albeit lower than MRI, ultrasound, and fluorescence imaging. In addition to safety issues associated with radiation exposure, one of the disadvantages of PET is the need for a cyclotron to produce most PET isotopes. SPECT isotopes have relatively longer half-lives and are more accessible. Another challenge of PET is that the chemical coupling of the PET radionuclide to proteins and nanomaterials is often difficult. This problem has been recently alleviated by the introduction of modular chemical approaches, such as “click” chemistry and small molecule conjugates [9]. The technical advances in the production of longer-lived PET radioisotopes, such as ^{124}I, make these probes more readily available for clinical and research use.

3.2 MRI

Magnetic resonance imaging (MRI) uses non-ionizing radiation generated from an electro-magnetic field to acquire images with high spatial resolution (sub-millimeter), temporal resolution, and excellent soft tissue contrast. It typically relies on the detection of the relaxation properties (T_1 and T_2) of excited hydrogen (^{1}H) nuclei in water and lipids of soft tissue. The major disadvantage of MRI in molecular imaging is its relatively low sensitivity (10^{-3} to 10^{-9} M). In addition, tissues with low water density, such as pulmonary tissue, are poorly visible by ^{1}H-MRI. Targeted contrast agents are employed to allow accumulation of sufficiently high concentrations (microgram to milligram quantities) of MRI probes in the target tissue needed to achieve high signal-to-noise ratios. Nanoparticles with relatively high payloads of paramagnetic materials like iron oxides (T_2 contrast agent) or gadolinium (Gd^{3+} Gd^{3+})-chelates (T_1 contrast agent) are often used as MRI contrast agents. Ultrasmall gadolinium oxide (Gd_2O_3) nanoparticles have been getting attention recently for having approximately a 4-fold increase in water relaxivity compared to values for Gd^{3+}-chelates [10]. Clinical studies do not reveal overt toxicity of iron oxide particles [11], and while gadolinium in its unbound (“free”) state is highly toxic, Gd^{3+} is generally considered safe when administered in chelated form [12]. An alternative platform for targeted MRI contrast agents are biocompatible perfluorocarbon (PFC) nanoparticles enriched in fluorine-19 (^{19}F) for detection by ^{19}F-MRI. The paucity of endogenous ^{19}F in biological tissue allows for highly specific and quantifiable detection of the fluorine signature of PFCs with no interference from a background signal [13]. This concept has since been evaluated with targeted PFC nanoparticles *in vivo* [14]. PFC nanoparticles can also be surface functionalized with up to 10,000 Gd^{3+}-chelates per particle allowing for sensitive ^{1}HMR imaging *in vivo* [15]. Recent studies have demonstrated that Gd^{3+} enhanced the ^{19}F signal of these particles nearly four-orders of magnitude, allowing for the potential detection of nanomolar levels of the Gd^{3+}-labeled PFC nanoparticles [16].

3.3 Ultrasound Imaging

The great advantage of ultrasound (US) imaging is that it is widely available, inexpensive, and portable, and it is currently the most widely used clinical diagnostic system for cardiac imaging. Molecular imaging with US relies on targeted micron-sized particles or nanoparticles as contrast agents that produce an ultrasound signal in response to ultrasonic frequencies. Gas-filled microspheres ("microbubbles") have particle sizes that typically range from 2.5 to 5 μm [17], and are most commonly composed of PFC or nitrogen gas encapsulated by shells made of phospholipid, albumin, or biodegradable polymers [18]. Acoustically reflective particles also include those with gas- or liquid-filled cores, such as echogenic liposomes (ELIPs) (micron- or nano-sized), and PFC nanoparticles. The sensitivity of US systems has been reported as high as 10^{-9} M [19]. This seemingly high sensitivity is contrasted with the limited imaging depth of penetration of ultrasonic waves (1–200 mm). Just as sensitivity decreases with imaging depth, so does the image resolution. New and advanced US imaging platforms work to address issues of sensitivity and resolution. One such system often used in preclinical animal imaging is intravital catheter-based ultrasound microscopy (IVUS) that achieves highly resolved anatomical structures of deeper vascular beds that can be merged with contrast distribution. Sensitivity of US systems can also be improved by engineering contrast agents targeted to specific endothelial targets so that the signal can persist and intensify in the target tissue. Seeing as both the neovasculature and extravascular space can display inflammatory markers, the targeted-microbubble approach is somewhat limited because their circulation and distribution is restricted to the intravascular space. This would necessitate the need for nano-sized targeted contrast agents that can exit large blood vessels by virtue of their size, and allow detection and quantification of neovascular and extravascular targets *in vivo* [20]. However, nanoscale targeting strategies in US molecular imaging are challenging. The frequencies used to detect gaseous PFC nanobubbles can cause them to cavitate and rupture, although nongaseous PFC nanoparticles are stable to heat, pressure and shear forces [17]. Nanoparticle contrast agents (gas- and liquid-filled) can also have little inherent echogenicity in response to ultrasound, and therefore provide poor signal relative to background when in circulation [21]. Interestingly, when PFC nanoparticles are bound on the surface of target tissue, they create a focal sound impedance that produces a strong ultrasound signal without an accompanying increase in background signal [22].

3.4 Fluorescence imaging

Optical imaging using fluorescence detection systems is a powerful imaging method in small animals due to their sensitivity and fast acquisition and image processing times, thus allowing for high-throughput imaging in real-time. *In vivo* fluorescence imaging using fluorophores emitting energy in the visible range (450–650 nm) remains limited due to the significant absorption and scattering of emitted photons, and the autofluorescence of background tissue, all reducing target-to-nontarget ratio. Fluorophores emitting in the near-infrared (NIR) spectrum (650–900 nm) have greater sensitivity due to better transmission and detection of the emitted light in picomolar to femtomolar concentrations (10^{-12} to 10^{-15} M) [23]. Although quantitative optical depth-resolved NIR fluorescence systems are routinely available for mice, the fundamental limitation of optical imaging in human will be the limited depth of penetration of the photon signal. Fluorescence-mediated molecular 3D tomography (FMT), and intravital microscopy (IVM) are both being explored for studying molecular processes in animal studies. IVM may only focus on small areas of interest, but it is highly sensitive for imaging molecular and cellular processes in intact living tissues with high resolution (1–10 μm) [24]. Fluorescence-Assisted Resection and Exploration (FLARE™) is a new NIR fluorescence imaging platform designed for real-time, non-contact image-guided surgery that is going through the clinical translational process for new medical imaging devices [25].

3.5 Multimodality imaging

Multimodality imaging probes contain two or more complementary imaging components that allow for their detection and localization by complimentary imaging technologies. In combining the advantages of different imaging techniques, multimodal nanoparticles have the potential to overcome the sensitivity or resolution limitations that a single imaging approach may have. The advantages of such probes, as well as their limitations have been recently reviewed [9].

The use of multiple imaging modalities is often required for molecular probes that are typically seen as `hot spots.' With limited information about the precise anatomical location and physiology of the organ, quantification of *in vivo* probe concentration, as defined by a region- or volume-of-interest, is challenging. Hybrid modalities such as PET or SPECT systems fused with computed tomography (CT) scanners offer the possibility to integrate highly sensitive PET/SPECT images with high-resolution morphological images provided by CT to obtain an anatomic distribution of the probe. It has also been demonstrated that the integration of PET and MRI provides the high spatial resolution of MRI and the high sensitivity and functional imaging of PET [26]. Three-dimensional scanning techniques are also likely to help co-registration of ultrasound and optical imaging technologies.

In recent years, multiple groups have highlighted the potential of multimodal probes for MRI and PET [27], MRI and fluorescence [28], and MRI, PET and fluorescence [29] in imaging inflammation *in vivo*. In the subsequent sections, we will briefly describe various types of nanoparticle platforms available and highlight how multifunctional nanoparticles can be designed for both multimodal diagnostic imaging and drug delivery capabilities.

4. Nanocarriers for targeting imaging agents and drugs to activated endothelium

Nanoparticles of diverse shape, materials and physical properties are designed to identify sites of pathology and deliver therapeutics to these sites (Figure 3). Nanoparticles are especially attractive for the molecular imaging of vascular inflammation, since markers of activated endothelium are readily accessible for circulating nanomaterials. Advantages of using nanocarriers include: (1) the ease of particle functionalization with antibodies or affinity peptides binding to CAMs or another appropriate marker of inflammation; and (2) the ability to deliver a higher concentration of contrast agent for every targeted binding event to achieve higher detection sensitivity of otherwise prohibitively sparse antigens. The enhanced selectivity and sensitivity of nanoparticle probes permit imaging of relatively subtle inflammatory changes in the vasculature.

When desirable, nanocarriers can extend the circulation for encapsulated versus free drugs and probes. First, stealth nanocarriers can elude clearance from the renal system and/or reticuloendothelial system (RES; i.e. liver, spleen, and bone marrow), which in turn enhances bioavailability. Second, agents encapsulated in carriers are protected from biodegradation [30]. From another perspective, encapsulation in carriers protects the body against toxic effects of drugs and imaging agents. Taken together, loading drugs or imaging probes in nanocarriers enables higher payload delivery compared to single molecules with reduced risk for off-target effects.

4.1 Nanoparticle properties

The biodistribution and clearance of nanocarriers is dictated by their size and shape, chemical composition, surface charge, avidity, and the density of targeting moieties. These parameters are discussed below.

4.1.1 Size—Nanocarriers are generally defined as objects having at least one dimension in the 1–100 nanometer scale, although some sources include dimensions less than 500 nm as nano-sized.1 By virtue of their small size, nanoparticles have high surface area to volume ratios. This provides both an abundant surface area for particle decoration for the purpose of targeting and drug/probe coupling, and an internal volume capable of encapsulating drugs or imaging agents. The internal volume increases cubically as external surface area is squared; with non-spherical nanocarriers, this relationship changes. For example, changes in a filamentous carrier's volume and surface area are more impacted by changes in radius than length.

As an example of the effects of size on nanoparticle behavior *in vivo*, researchers demonstrated the dependence of size on circulation retention, pharmacokinetics and permeability using Gd-based MRI contrast agents of varied size ranges under 20 nm: polyamidoamine (PAMAM) dendrimers with diameters less than 3 nm moved across vascular walls via endothelial barrier, dendrimers from 3 to 6 nm showed rapid renal clearance, those with 7–12 nm remained in circulation, whereas dendrimers larger than 12 nm underwent rapid liver and splenic uptake [31]. Frangioni's group has confirmed the relationship of nanoparticle size and tissue distribution with ^{99m}Tc-labeled fluorescent QDs by intraoperative fluorescence imaging and -scintigraphy [32]. Using QDs with discrete hydrodynamic diameters (HD) increasing from 4.36 nm to 8.65 nm, they found that QDs with HD < 5.5 nm result in rapid renal clearance of the QDs 4 hour post-intravenous (iv) administration. QDs larger than 5.5 nm had predominantly hepatic uptake. In general, compared to micron-size carriers, nano-scale carriers have more prolonged circulation and enhanced cellular uptake.

4.1.2 Shape—Carrier shape also modulates its circulation, and cellular uptake kinetics. Elongated filamentous polymer particles, as reported by Discher *et. al.* have extended circulation times compared to spherical nanoparticles, probably due to increased capacity to align with blood flow [33]. DeSimone's group have developed, by lithographic methods, nano- and micron-sized particles of uniform size, shape, and surface chemistry, revealing that non-spherical particles, rods in particular, as large as 3 μm (a size restrictive in the cellular uptake of spherical particles), are rapidly endocytosed by cultured epithelial cells [34]. Particle shape influences binding and phagocytosis by macrophages independently. The Mitragotri group compared binding and uptake of spheres, prolate ellipsoids, and oblate ellipsoids to macrophages in culture. They reported that while the attachment of prolate ellipsoids was greatest among the particle types and four times greater than spheres, a greater percentage of oblate ellipsoids are internalized once bound. Although the spherical particles bound in lesser numbers than either ellipsoid types, both the spheres and the oblate ellipsoids were more highly internalized than the prolate ellipsoids. These relationships existed for particles in a specific volume range (0.075–0.69 mm^3), and differences in phagocytosis were not observed in larger volumes [35]. Decoration of carriers with affinity ligands further modulates role of carrier geometry. For example, Muro *et. al* found that large ICAM-targeted polymer discs (0.1 × 1.0 × 3.0) μm had more specific targeting and less non-specific tissue uptake but slower rates of endothelial endocytosis compared to 100 nm spheres targeted to the same CAM molecule [36].

4.1.3 Surface functionalization—Manipulating the carrier's surface charge, solubility and affinity through the inclusion of coating materials and reactive groups greatly modulates

[1]National Institutes of Health and the National Science Foundation define nanoparticles as having at least one dimension between 0.1–100 nm. The National Heart, Lung, and Blood Institute defines biomedical nanoparticles to be less than 300 nm, and European institutes set a bar at 500 nm. A commonly held convention contends that a nano-size structure contains at least one dimension smaller than 1 micron.

their targeting. Nanoparticle surface charge can affect serum protein binding and non-specific adhesion to cells. Generally, neutral and slightly negatively charged carriers have longer circulation times and less non-specific binding. The introduction of biocompatible hydrophilic polymer chains, such as PEG, creates a hydrated brush-like coating that enhances nanoparticle solubility, prolongs blood circulation times, and delays RES clearance. For instance, PEG-coated liposomes have circulation times orders of magnitude longer than uncoated liposomes [37]. This "stealth" approach has since been adapted to improve biocompatibility and control pharmacokinetics of diverse carrier types [38]. A comparison of linear- versus star-shaped polymer nanostructures with PEG chains of varied lengths and radiolabeled with ^{64}Cu for PET imaging of mice demonstrated clearly that star-shaped nanostructures with longer PEG chains (MW 5 kDa vs 2 kDA) were retained in the blood longer and had lower hepatic and splenic uptake. Linear-shaped nanocarriers of equivalent chemical composition were rapidly cleared through renal excretion. The size (25 to 70 nm) and the core composition of the star-shaped structures were shown to have less impact on circulation time than the length of the PEG chains [39].

The longer plasma half-life of PEGylated nanoparticles can lead to increased background signal during image acquisition, which can be offset by exploiting the PEG-chains as sites for introducing targeting moieties. The extension of flexible PEG or PEG-like molecules distal to a nanoparticle surface provides optimal conjugation sites for targeting molecules. Targeting moieties introduced at the flexible termini improve the accessibility of the ligand to tissue antigens for enhancing nanoparticle affinity while preserving stealth features [37]. Particle functionalization can also be achieved by chemical modifications to the particle surface material itself. These modifiable sites are important for accessorizing particles with: (i) targeting vectors like antibodies and peptides; (ii) contrast agents such as radionuclides [40], NIR-dyes [41], and MRI-active metal-chelates [42]; and (iii) therapeutic agents. Introduction of amines, carboxylic acids, and azides are commonly used modular approaches for nanocarrier coupling to ligands [43]. Activation of sulfhydryl and thiol groups also creates linking capabilities with proteins, peptides, and small molecules [43].

4.2 Nanoparticle types for imaging and drug delivery

4.2.1 Liposomes and lipid-based nanoparticles—Liposomes are the earliest and most extensively developed drug delivery carriers studied since the 1960s. Liposomes are self-assembled bi-layer vesicles generated from the interaction of phospholipids with aqueous media (Figure 3). Soluble drugs can be loaded in the aqueous core, and hydrophobic drugs partitioned into the lipid bi-layer. Liposomes with sizes between 50–200 nm and with bi-layer membranes between 3–5 nm thick are suitable for targeted vascular drug delivery and imaging purposes [44].

While most research related to liposomes is in the area of drug delivery as reviewed elsewhere [45], there are many examples of their utility as imaging agents. Acoustic liposomes or ELIPs for US imaging can be different from their drug delivery counterparts in that only certain compositions of lipid dispersions become echogenic following lyophilization. Although the detailed structure of ELIPs is unknown, it is generally recognized that echogenicity of these particles is probably due to air trapped in the lipid layers during rehydration of the lyophilized preparation [46]. There exist many recent examples of immuno-targeted ELIPs for US imaging [47, 48]. Paramagnetic liposomes for MRI were first introduced in the 1980s, and new generations are designed to enhance the MRI signal by modulating the membrane fluidity by changing phospholipid chain length, saturation and head group size [49]. Recent examples include Gd^{3+}-loaded ^{111}In-labeled liposomes targeted to the low-density lipoprotein receptor (LDLR) that enabled both MRI imaging and SPECT/CT imaging of atherosclerotic plaques in both LDLR deficient mice

(*ldlr*−/−) and *apoE*−/− deficient mice [50]. Liposomes labeled with radioisotopes have been used for PET [51] and SPECT imaging [52]. The most significant challenge to liposome radiotracing has been finding ways to increase radiolabel stability in the liposomal formulation. The most stable direct-labeling of pre-formed liposomes, referred to as „afterloading,' is accomplished by chelation methods that result in the radionuclide being anchored to the lipid bilayer or within the aqueous core of the liposome. Long circulating liposomes with the label incorporated in the lipid bilayer, using ^{18}F-labeled diglycerides such as 3-[^{18}F]fluoro-1,2-dipalmitoyl glycerol ([^{18}F]FDP), show steady circulation in rats over 90 min by PET imaging. The liposomal formulations have decreased retention in liver, spleen and lung when compared to free [^{18}F]FDP [51].

4.2.2 Polymer-based nanoparticles—Polymersomes (diameters 100–600 nm) are vesicles analogous to liposomes self-assembled from block copolymers combining hydrophilic and hydrophobic moieties. With a membrane thickness of about 8 nm, the polymersome membrane is more than twice as thick as that of the liposome membrane; hence polymersomes are more durable than liposomes. Furthermore, inclusion of more than 15 mol % of PEG in liposomal phospholipids destabilizes the bi-layer membrane, whereas amphiphilic copolymers forming polymersomes can contain PEG in every polymer chain thus allowing for complete surface coverage of the vesicle; hence polymersomes are fully stealthy. Molecular self-assembly of polymers will also produce polymer micelles (i.e. monolayered vesicles), appropriate for small hydrophobic cargoes, and long filaments of micelles called worm micelles or filomicelles. Particle morphology and size, among other properties, are dictated by the ratio of the hydrophobic polymer (e.g. polylactic acid, PLA; polylactic-co-glycolic acid, PLGA; polyethylimine, PEI) to the hydrophilic PEG [53].

While the previously discussed nanocarriers form by thermodynamically-driven self-assembly mechanisms, other polymer nanoparticles form through processing. Polymer nanoparticles (PNC), with size ranging from 50 to 600 nm, can be formed through homogenization of emulsion phases, gas expansion, or solvent extraction techniques [7]. High-energy emulsions of phases allow for inclusion of hydrophobic and hydrophilic domains in an amphiphilic polymer matrix, but encapsulation of proteins is more challenging because of their inactivation. However, recent methods have been described to load active antioxidant enzymes, like 250 kDa catalase, into PEG-PLGA PNCs, and protect them from proteolysis. Using PEG-catalase instead of naked enzyme further facilitates encapsulation and protection against external proteases [54]. Conjugation of antibodies to PECAM provides targeting of such PNC to endothelial cells in vitro and in animals PNCs. Filamentous PNC loaded with active catalase can be formed using the same technique when the PEG fraction in the block copolymer is reduced to less than 20 % [30].

4.2.3 Magnetic nanoparticles—Long used for MRI, magnetic nanoparticles (MNPs) are useful in numerous *in vivo* applications for molecular imaging. MNPs are typically composed of a superparamagnetic core, often iron oxide, surrounded by a stabilizing, biocompatible surface coating such as dextran, siloxane, oleic acid or other hydrophilic molecules [55, 56]. The nomenclature for MNPs formulations are classified based in their size as follows: (i) micrometer-sized paramagnetic iron oxide (MPIO; several microns), (ii) super-paramagnetic iron oxide (SPIO; hundreds of nm), and (iii) ultrasmall superparamagnetic iron oxide (USPIO; less than 50 nm). USPIOs with a single core include monocrystalline iron oxide particles (MION; core diameter 3 nm) and cross-linked iron oxide particles (CLIO; core diameter 30 nm), and they have low relaxivities due to their small cores [57]. However, an important development in making MNPs suitable for clinical studies and other biomedical applications was the stabilization of the dextran coating through cross-linking. As such, dextran-stabilized CLIOs, with pendant amine groups, are non-immunogenic, biodegradable and easily functionalized, and thus has emerged as a

platform for clinical molecular imaging applications [58]. Approaches for functionalization of MNP surfaces through PEG, and PEG-like polymers, phospholipids and copolymers have been recently comprehensively reviewed [56]. Many groups have studied the use of heterobifunctional PEG which can be covalently bound to the SPIO surface and also bind a targeting or imaging moiety to the distal end of the PEG [56, 59]. Magnetite-based MNPs containing catalase and SOD, potent anti-oxidant enzymes, have been synthesized using a controlled precipitation reaction of calcium oleate in the presence of a ferrofluid stabilized by a surfactant copolymer Pluronic F127. These magnetically responsive larger carriers (~300–400 nm) successfully loaded active enzyme (20–33 % efficiency) and shielded the enzymes from degradation by proteolytic enzymes. Magnetically directed MNPs containing catalase protected cultured endothelial cells from cell death from oxidative damage resulting from high concentration hydrogen peroxide exposure [60].

4.2.4 Perfluorocarbon (PFC) nanoparticles—PFC nanoparticles have found applications in US, MRI, and SPECT molecular imaging, in addition to demonstrating drug delivery capabilities. Nanoscale PFC particles are typically lipid- or surfactant-stabilized nanodroplets of PFC created by self-assembly and emulsion techniques [61]. Sizes for PFC nanoparticles generally range from 200 nm to 250 nm [17, 20]. As with other nanocarriers, the particle surface can be functionalized to accommodate targeting moieties, imaging agents, or therapeutics payloads (Figure 3). As with liposomes, materials can be noncovalenty associated with the surface, and dissolved in the coating layer. For example, Soman *et. al.* incorporated melittin, a membrane penetrating amphipathic peptide, into the outer lipid layer of PFC nanoparticles to demonstrate the potential of PFC particles as nanocarriers of cytolytic peptides [62]. Different PFCs can be used in the liquid core, including perfluorodichlorooctane, perfluoro 15-crown-5-ether, and most commonly, perfluorooctyl bromide (PFOB). In the PFOB nanoparticle systems described by Lanza, Wickline and colleagues, the liquid PFC core represents 98% of the total particle volume, affording a substantial ^{19}F concentration (~100 M) [61, 63] for sensitive detection by MRI techniques.

4.2.5 Dendrimers—A dendrimer is a 3D macromolecule composed of branched monomers that radiate outwards from a central core (Figure 3). Dendrimers are typically synthesized step-wise from the core layer upon layer. The resulting branched polymeric structures have layered architectures that enable regional functionalization and provide versatility in design for biomedical applications. Dendrimers are formed from a variety of polymers, most commonly polyamidoamine, polyesters, polyethers, and polypeptides [64]. The end-group density of the outermost region of a dendrimer is dictated by the number of branch points or generations of the dendrimers. At the fourth generation, dendrimers may become globular or spherical; typically the largest most complex dendrimers are possible at the tenth generation producing a maximum diameter of about 10 nm. Highly branched dendrimers provide densely associated, multivalent terminal units useful to concentrate drug payloads or imaging agents. Dendrimers built from aliphatic polyester dendrons have been recently reported for dynamic SPECT imaging using rats. Parrott *et. al.* labeled the dendrimers with ^{99m}Tc at generations 5–7 by metalation, using amidation chemistry with a tridentate bis(pyridyl)amine ligand creating region-specific labeling of the dendrimers. SPECT images correlated well with biodistribution data, and the dendrimers were rapidly cleared from the bloodstream with no evidence of toxicity [65].

4.2.6 Quantum dots—Made from semiconductor materials (e.g. CdSe, CdS, CdTe. ZnS, PbS, and alloys) overlaid with a coating of ZnS (Figure 3), QDs are stable (unless exposed to UV irradiation), and bright light-emitting particles with core diameters ranging from 2 to 10 nm. QDs provide a more sharp fluorescent signal in comparison to other probes, and they

resist photobleaching. Their emission spectra are tunable by particle size and composition and are available in ranges from 500–800 nm. Although issues with biocompatibility have prevented clinical imaging applications of QD research to date, there are promising developments in QD core coating, surface chemistry, and functionality. Colloidal synthesis of QDs creates more biocompatible products and lends itself best to translational biomedical applications. PEG coating enhances biocompatibility of QDs and enables vascular targeting through ligand-functionalized PEG [66]. In addition to PEG, amphiphilic polymers, proteins and polyethyleneimine have been used to coat QDs in order to improve biocompatibility and convert the immiscible, hydrophobic surface of QDs to hydrophilic particles without affecting the fluorescence quantum yield [67].

5. Endothelial-targeted nanocarriers for imaging of vascular inflammation *in vivo*

As alluded to in section 1.1, cell adhesion molecules (CAMs) are attractive candidates for targeted delivery of nanocarriers to activated endothelium in vascular pathology. In this section, we will specifically highlight the potential of VCAM-1-, ICAM-1-, and selectin-targeted nanocarriers as diagnostic probes for imaging of vascular inflammation in animal studies.

5.1 VCAM-1

The potential of VCAM-1-targeted nanoparticles as diagnostic agents for vascular inflammation was first described by Weissleder *et. al.* using 35 nm CLIO magneto-optical particles targeted with anti-VCAM Ab. Focal inflammation in a mouse ear was induced with a subcutaneous injection of tumor necrosis factor (TNF) cytokine. Intravital microscopy of VCAM-targeted CLIOs administered iv 24 h post-insult, revealed their accumulation at the site of inflammation. Probe accumulation was maximal at 6 h post-injection (p.i.) [68]. As an alternative to Ab-targeting, several generations of VCAM-1 targeting peptides with homology to VLA4, a natural ligand of VCAM-1, have been identified by phage display and coupled to the magneto-optical CLIO particles [69, 70]. The first peptide identified, termed VP, has 12-fold higher binding to VCAM-1 relative to anti-VCAM-1 Ab *in vitro* [69]. IVM of VP bound to CLIOs (VNP) in the TNF-induced ear inflammation mouse model confirmed targeting and specificity to VCAM-1 in the inflamed tissue relative to control particles and non-inflamed tissue. These results were further confirmed by *in vivo* MRI studies with apolipoprotein E-deficient mice (*apoE*−/−) predisposed to atherosclerosis under a high-cholesterol diet (HCD). In this model, VNP could identify aortic atherosclerotic plaques using MRI, as evidenced by the significant increase in contrast-to-noise ratio after VNP injection. To enhance targeting to VCAM-1, the same group identified another linear peptide affinity ligand homologous to VLA4, that when bound to magneto-optical CLIOs (VINP-28) exhibited 20-fold higher binding to VCAM-1 *in vitro* than VNP [70]. *In vivo* IVM and MRI confirmed specific binding of VINP-28 particles to inflamed tissue (in both the TNF-induced ear inflammation model and in the aortic arch of *apoE*−/− mice + HCD). MRI signal contrast due to VINP-28 uptake was reduced to pre-contrast baseline levels when mice were given 8 weeks of therapeutic chlolesterol-lowering statin treatment [70].

Choudury *et. al.* have assessed the potential of larger 1 μm MPIO particles targeting to VCAM-1 in mouse models of cerebral inflammation. MRI detected enhanced uptake of anti-VCAM-1 Ab-coated MPIO in a mouse model of acute TNF-induced inflammation in the brain, blocked by pre-injection with anti-VCAM-1 Ab, validating probe specificity [71]. These same MPIO-Ab particles were injected iv in a mouse 3 h post cerebral ischemia/reperfusion model and localized to the damaged brain significantly higher than untargeted particles, differentiating normal tissue from damaged tissue [72].

Using the PFC ^{19}F NMR nanoparticle imaging platform, 250 nm VCAM-1-targeted PFC nanoparticles were used to detect renal inflammation in *apoE*−/− mice, and provided a 4-fold increase of MR signal in the kidneys relative to untargeted particles. This targeting correlated with the increase in VCAM-1 expression in the organ [73]. In addition to MRI-based detection methods, VCAM-1 targeted microbubbles [74] and liposomes [47] are also available for plaque imaging using US.

5.2 ICAM-1

ICAM-1 is another endothelial cell adhesion molecule that is up-regulated during vascular inflammation. Recently, ^{64}Cu-labeled latex nanoparticles (NPs) coated with anti-ICAM have been used for PET imaging of pulmonary inflammation caused in mice by systemic (i.p.) injection of bacterial lipopolysaccharide (LPS). ^{64}Cu-DOTA-labeled IgG tracing showed that approximately 200 anti-ICAM molecules are coupled per one particle with diameter of 100 nm. After iv injection of anti-ICAM/NPs, a 3–4-fold increase in radioactivity was observed in the lungs of LPS-challenged mice compared to control mice [75] (Figure 4). Due to the privileged perfusion and extended endothelial surface area in the alveolar capillaries, the lung is the preferential target of ICAM-targeted probes [76, 77]. ZnS QDs have been conjugated to anti-ICAM-1 Ab or anti-VCAM-1 Ab via bifuctionalized PEG to create ~100 nm QDs. One hour after iv administration of these targeted QD in diabetes-induced rats provided a 5-fold increase in vascular retinal fluorescence compared to control IgG-coated nanoparticles [66]. ELIPs have been used for ultrasound detection of ICAM-1 or VCAM-1 in atheromas in an atherosclerosis swine model. Ab-targeted ELIPs (500–800 nm) enhanced contrast in injured endothelium by nearly 40 % compared to untargeted particles and in control animals [47].

5.3 Selectins

E- and P-selectins are good targeting candidates due to low basal expression, which affords a low background signal. Imaging of selectin expression *in vivo* has been studied mostly with MRI and USPIO nanoparticles. MRI of TNF-induced inflammation of the mouse ear, with 30–50 nm USPIOs targeted with anti-E-selectin Ab, had contrast enhancement up to 18 h p.i. of USPIOs, and this contrast was sustained over 18 d. No changes in contrast were observed in control groups [78]. In a recent study, 25 nm USPIO MNPs were targeted to E-selectin in a rat model of traumatic brain injury. These targeted MRI agents carried a high-affinity heptapeptide binding to E-selectin, and they demonstrated a maximal signal enhancement over the uninjured hemisphere 70 min p.i., while non-targeted particles showed no difference. Interestingly, this difference in targeting was achieved with only 10 % coverage of the accessible particle surface with targeting ligand [79]. MRI-active GlycoNanoParticles (GNPs) formulated from 35 nm CLIO have been designed for the detection of E- and P-selectin in a multiple sclerosis rat model involving an acute brain inflammatory insult induced by interleukin-1β administration. These GNPs were designed to display 10^6 copies of the natural sLe^x glycan ligand directed to selectins. When injected 3 h post-insult, GNP-sLe^x accumulated in the inflamed lesions of the brain, with insignificant accumulation in the control animals. Compared to untargeted particles, selectin-directed GNP-sLe^x achieved nearly a 4-fold increase in localization [80]. MRI of post-stroke neuroinflammation was investigated with 50 nm iron oxide MNPs coated with P-selectin binding peptides (MNP-PBP) [81]. MNP-PBP were injected 24 h after ischemia/reperfusion brain surgery and allowed to circulate for 2 h before animals were imaged for particle localization. Targeted particles attenuated the MRI signal 35 % in infarcted tissue as compared to non-ischemic tissue, and at least 3-fold relative to untargeted particles.

6. Targeted nanocarriers for interventions in vascular inflammation

Delivering targeted anti-inflammatory drugs to reduce vascular inflammation may boost therapeutic effect while reducing adverse effects. For example, glucocorticoids are potent anti-inflammatory drugs, but adverse effects in non-targeted tissues include osteoporosis, obesity, and glaucoma [82]. Endothelial CAMs, molecules expressed in the inflamed vessels (which is verified and can be diagnosed using imaging probes as described above) have been explored to target therapeutics to the activated endothelium in a manner that will localize effects to the site of inflammation. This section will briefly outline targeting of anti-inflammatory agents, whereas more comprehensive reviews on targeting antioxidants can be found elsewhere [4, 83, 84].

6.1 VCAM-1

VCAM-1 is a promising determinant for targeting therapeutic nanoparticles specifically to activated endothelium. Liposomes targeted to VCAM-1 were investigated in *ldlr*−/− mice fed a hyperlipemic diet, a conventional animal model for atherosclerosis. Liposomes targeted using anti-VCAM Abs and formulated with an anti-inflammatory prostaglandin, PGE2, were administered daily for 2 weeks, and this was sufficient to rescue mice from outward signs of cardiovascular stress. The authors postulated that this formulation can also be protective in myocardial infarction or stroke, although this claim remains to be proven in appropriate animal models. However, targeted liposomal treatment reversed atherosclerotic lesions, and mice survived to old age despite being fed a high-fat diet. Untargeted liposomal formulations resulted in a 47 % decrease of accumulation within sites of inflammation, and drug alone did not reverse atherosclerotic lesions [85].

6.2 ICAM-1

ICAM-1 is normally expressed in the vasculature, yet its surface density enhances several fold in sites of inflammation [4]. Thus, ICAM-1-targeted nanocarriers can be used for both diagnostic and therapeutic applications [1, 77]. Even in naïve mice, 200 nm PNCs targeted to ICAM-1 with anti-ICAM Ab showed nearly a 30-fold increase in endothelial uptake relative to control IgG control particles [77]. This delivery system was further investigated to treat lysosomal storage diseases that are associated with vascular inflammation. ICAM-1-targeted PNCs were used to deliver a lysosomal replacement enzyme acid sphingomylinase *in vivo* and indicated over a 20-fold increase in targeting to the endothelium versus untargeted free enzyme alone [86]. Interestingly, ICAM-1 molecules recycle back to the endothelial plasmalemma after internalization of ICAM-targeted nanocarriers, thereby providing sustained intracellular delivery [87]. Muro *et. al.* highlight that targeting of nanocarriers to the endothelium via ICAM *in vitro* and *in vivo* can be modulated by controlling Ab surface density [88].

An alternative to delivering a therapeutic drug is to deliver stem cells to the site of injury with hope they can attenuate the progression of inflammatory diseases like atherosclerosis. A recent report demonstrated that ELIPs targeted to ICAM-1 can be used as both a US contrast agent for imaging and as a US-triggered controlled release delivery vehicle for vascular stem cells [89]. ELIPs loaded with vascular stem cells were studied *ex vivo*, in an atherosclerotic porcine model. Although ICAM-targeted ELIPs target specifically to the aortic endothelium, there was no difference in stem cell accumulation to the aorta relative to IgG-modified particles. However, US-triggered sonoporation of the liposome resulted in over a 2-fold increase in stem cell accumulation. This would suggest that sonoporation is required to enhance stem cell release and binding to the endothelium.

6.3 Selectins

Selectins are specific vascular targets soon after the onset of inflammation. In a glomerular endothelial inflammation model, anti-E-selectin Ab was used to target dexamethasone(Dex)-loaded liposomes (120 nm) to the renal endothelium. Targeting of liposomes resulted in 3.6-fold greater localization in inflamed kidneys compared to non-targeted IgG-coated liposomes. Furthermore, the targeted delivery of Dex lowered inflammatory markers by 60–70 % relative to controls, and side effects typically associated with bolus Dex were negligible for the targeted liposome formulation [90]. Another selectin-targeted liposomal intervention was used in a mouse auto-immune uveoretinitis model that is translatable to vascular inflammation diseases of the retina. Targeting of 100 nm liposomes to selectins was achieved with sLe^x-liposome conjugation (sLe^xL). The sLe^xL formulated with Dex, displayed selective accumulation at the inflamed eye within 5 minutes of iv injection versus a negligible accumulation of untargeted liposomes [91]. Gene expression profiling would suggest that genes are getting down-regulated with low dose Dex-loaded sLe^xL as compared to high dose Dex treatment alone. However, more extensive studies need to confirm that pro-inflammatory responses are decreasing in response to nanoparticle treatment.

7. Conclusions and future directions

Studies of the past decade highlight the potential of CAM-targeted nanocarriers as diagnostic agents and drug delivery vehicles for numerous inflammation-driven diseases. With advancements in imaging technology, including hybrid scanners, and the development of refined nanocarrier platforms that take advantage of favorable chemistry, we foresee a new generation of multifunctional nanoparticles. Furthermore, with the discovery of new affinity ligands to molecular signatures of inflammation, there will undoubtedly be new imaging targets to exploit for both diagnosis and therapy. Work is also underway in dual nanoparticle-targeting of different CAM combinations to increase adhesion strength to the target compared to single-epitope targeted particles [92, 93].

In summary, endothelial targeted probes and therapeutics hold much promise in the management of disease conditions involving vascular inflammation. However, the field is still in its adolescence. Considerable challenges remain on optimizing nanocarrier geometry and surface properties to promote the most effective targeting and drug delivery strategies while minimizing non-specific tissue residence times. Translation of these novel nanomedicine devices to the clinic will be exciting and challenging, due to their inherent complexity. Meanwhile, using these targeted nanodevices in animal models as precise diagnostic tools and as specific interventions for inflamed endothelium holds promise in extending our knowledge of pathological mechanisms of inflammatory disease.

Acknowledgments

This work was supported by National Institutes of Health grants HL087036, HL073940 and HL091950.

References and recommended reading

• of special interest

•• of outstanding interest

[1]. Muzykantov VR. Targeting of superoxide dismutase and catalase to vascular endothelium. J Control Release. 2001; 71:1–21. [PubMed: 11245904]

[2]. Simone E, Ding BS, Muzykantov V. Targeted delivery of therapeutics to endothelium. Cell Tissue Res. 2009; 335:283–300. [PubMed: 18815813]

[3]. Christofidou-Solomidou M, Muzykantov VR. Antioxidant strategies in respiratory medicine. Treat Respir Med. 2006; 5:47–78. [PubMed: 16409015]

[4••]. Muro S, Muzykantov VR. Targeting of antioxidant and anti-thrombotic drugs to endothelial cell adhesion molecules. Curr Pharm Des. 2005; 11:2383–401. [PubMed: 16022673] A comprehensive review on the role of endothelial cell adhesion molecules (CAMs) in vascular disease and the potential of CAMs in targeting antioxidant and anti-thrmobotic nanomedicines.

[5]. Kluger MS. Vascular endothelial cell adhesion and signaling during leukocyte recruitment. Adv Dermatol. 2004; 20:163–201. [PubMed: 15544200]

[6]. Almenar-Queralt A, Duperray A, Miles LA, Felez J, Altieri DC. Apical topography and modulation of ICAM-1 expression on activated endothelium. Am J Pathol. 1995; 147:1278–88. [PubMed: 7485391]

[7]. Ding BS, Dziubla T, Shuvaev VV, Muro S, Muzykantov VR. Advanced drug delivery systems that target the vascular endothelium. Mol Interv. 2006; 6:98–112. [PubMed: 16565472]

[8]. Dobrucki LW, Sinusas AJ. PET and SPECT in cardiovascular molecular imaging. Nature reviews. 2010; 7:38–47.

[9••]. Louie A. Multimodality Imaging Probes: Design and Challenges. Chem Rev. 2010; 110:3146–95. [PubMed: 20225900] A recent review highlighting the design of nanoparticles for multimodality imaging, including the different approaches for incorporating contrast agent to the nanaoparticle of varing structure and composition.

[10]. Ahren M, Selegard L, Klasson A, Soderlind F, Abrikossova N, Skoglund C, et al. Synthesis and characterization of PEGylated Gd2O3 nanoparticles for MRI contrast enhancement. Langmuir. 2010; 26:5753–62. [PubMed: 20334417]

[11]. Weissleder R, Stark DD, Engelstad BL, Bacon BR, Compton CC, White DL, et al. Superparamagnetic iron oxide: pharmacokinetics and toxicity. AJR Am J Roentgenol. 1989; 152:167–73. [PubMed: 2783272]

[12]. Penfield JG, Reilly RF Jr. What nephrologists need to know about gadolinium. Nat Clin Pract Nephrol. 2007; 3:654–68. [PubMed: 18033225]

[13]. Caruthers SD, Neubauer AM, Hockett FD, Lamerichs R, Winter PM, Scott MJ, et al. In vitro demonstration using 19F magnetic resonance to augment molecular imaging with paramagnetic perfluorocarbon nanoparticles at 1.5 Tesla. Invest Radiol. 2006; 41:305–12. [PubMed: 16481914]

[14]. Neubauer AM, Caruthers SD, Hockett FD, Cyrus T, Robertson JD, Allen JS, et al. Fluorine cardiovascular magnetic resonance angiography in vivo at 1.5 T with perfluorocarbon nanoparticle contrast agents. J Cardiovasc Magn Reson. 2007; 9:565–73. [PubMed: 17365236]

[15]. Anderson SA, Rader RK, Westlin WF, Null C, Jackson D, Lanza GM, et al. Magnetic resonance contrast enhancement of neovasculature with alpha(v)beta(3)-targeted nanoparticles. Magn Reson Med. 2000; 44:433–9. [PubMed: 10975896] Gd-loaded PFC nanoparticles for enhanced ^{1}H MRI are described for the first time.

[16•]. Neubauer AM, Myerson J, Caruthers SD, Hockett FD, Winter PM, Chen J, et al. Gadolinium-modulated ^{19}F signals from perfluorocarbon nanoparticles as a new strategy for molecular imaging. Magn Reson Med. 2008; 60:1066–72. [PubMed: 18956457] This paper highlights the first demonstration of relaxation enhancement of ^{19}F MRI signals from PFC-Gd nanoparticle preparations as modulated by Gd. The Gd enhances the ^{19}F nuclei signal 125% which increases the sensitivity of the imaging probe for *in vivo* applications.

[17]. Tran TD, Caruthers SD, Hughes M, Marsh JN, Cyrus T, Winter PM, et al. Clinical applications of perfluorocarbon nanoparticles for molecular imaging and targeted therapeutics. Int J Nanomedicine. 2007; 2:515–26. [PubMed: 18203420]

[18]. Villanueva FS. Molecular imaging of cardiovascular disease using ultrasound. J Nucl Cardiol. 2008; 15:576–86. [PubMed: 18674725]

[19]. Sinusas AJ, Bengel F, Nahrendorf M, Epstein FH, Wu JC, Villanueva FS, et al. Multimodality cardiovascular molecular imaging, part I. Circ Cardiovasc Imaging. 2008; 1:244–56. [PubMed: 19808549]

[20]. Marsh JN, Partlow KC, Abendschein DR, Scott MJ, Lanza GM, Wickline SA. Molecular imaging with targeted perfluorocarbon nanoparticles: quantification of the concentration

dependence of contrast enhancement for binding to sparse cellular epitopes. Ultrasound Med Biol. 2007; 33:950–8. [PubMed: 17434667]

[21]. Hughes MS, Marsh JN, Hall CS, Fuhrhop RW, Lacy EK, Lanza GM, et al. Acoustic characterization in whole blood and plasma of site-targeted nanoparticle ultrasound contrast agent for molecular imaging. J Acoust Soc Am. 2005; 117:964–72. [PubMed: 15759715]

[22]. Lanza GM, Wallace KD, Scott MJ, Cacheris WP, Abendschein DR, Christy DH, et al. A novel site-targeted ultrasonic contrast agent with broad biomedical application. Circulation. 1996; 94:3334–40. [PubMed: 8989148]

[23]. Weissleder R, Ntziachristos V. Shedding light onto live molecular targets. Nat Med. 2003; 9:123–8. [PubMed: 12514725]

[24]. Hueber AJ, Stevenson R, Stokes RJ, Graham D, Garside P, McInnes IB. Imaging inflammation in real time--future of nanoparticles. Autoimmunity. 2009; 42:368–72. [PubMed: 19811304]

[25]. Gioux S, Choi HS, Frangioni JV. Image-guided surgery using invisible near-infrared light: fundamentals of clinical translation. Mol Imaging. 2010; 9:237–55. [PubMed: 20868625]

[26•]. Judenhofer MS, Wehrl HF, Newport DF, Catana C, Siegel SB, Becker M, et al. Simultaneous PET-MRI: a new approach for functional and morphological imaging. Nat Med. 2008; 14:459–65. [PubMed: 18376410] The authors report one of the first examples of targeted nanoparticles for multi-modal PET-MRI imaging.

[27]. Jarrett BR, Gustafsson B, Kukis DL, Louie AY. Synthesis of ^{64}Cu-labeled magnetic nanoparticles for multimodal imaging. Bioconjug Chem. 2008; 19:1496–504. [PubMed: 18578485]

[28]. Oostendorp M, Douma K, Wagenaar A, Slenter JM, Hackeng TM, van Zandvoort MA, et al. Molecular magnetic resonance imaging of myocardial angiogenesis after acute myocardial infarction. Circulation. 2010; 121:775–83. [PubMed: 20124125]

[29]. Nahrendorf M, Zhang H, Hembrador S, Panizzi P, Sosnovik DE, Aikawa E, et al. Nanoparticle PET-CT imaging of macrophages in inflammatory atherosclerosis. Circulation. 2008; 117:379–87. [PubMed: 18158358]

[30]. Dziubla TD, Shuvaev VV, Hong NK, Hawkins BJ, Madesh M, Takano H, et al. Endothelial targeting of semi-permeable polymer nanocarriers for enzyme therapies. Biomaterials. 2008; 29:215–27. [PubMed: 17950837]

[31]. Kobayashi H, Brechbiel MW. Nano-sized MRI contrast agents with dendrimer cores. Adv Drug Deliv Rev. 2005; 57:2271–86. [PubMed: 16290152]

[32]. Choi HS, Liu W, Misra P, Tanaka E, Zimmer JP, Itty Ipe B, et al. Renal clearance of quantum dots. Nat Biotechnol. 2007; 25:1165–70. [PubMed: 17891134]

[33]. Geng Y, Dalhaimer P, Cai S, Tsai R, Tewari M, Minko T, et al. Shape effects of filaments versus spherical particles in flow and drug delivery. Nat Nanotechnol. 2007; 2:249–55. [PubMed: 18654271]

[34•]. Gratton SE, Ropp PA, Pohlhaus PD, Luft JC, Madden VJ, Napier ME, et al. The effect of particle design on cellular internalization pathways. Proc Natl Acad Sci U S A. 2008; 105:11613–8. [PubMed: 18697944] Authors employ fabrication techniques to generate organic micro- and nanoparticles with complete control of size, shape, and surface chemistry. Evidence of particle internalization was obtained by using conventional biological techniques and transmission electron microscopy. They found that rod-like particles had increased internalization rates, analogous to rod-like bacteria.

[35]. Sharma G, Valenta DT, Altman Y, Harvey S, Xie H, Mitragotri S, et al. Polymer particle shape independently influences binding and internalization by macrophages. J Control Release. 2010; 147:408–12. [PubMed: 20691741]

[36•]. Muro S, Garnacho C, Champion JA, Leferovich J, Gajewski C, Schuchman EH, et al. Control of endothelial targeting and intracellular delivery of therapeutic enzymes by modulating the size and shape of ICAM-1-targeted carriers. Mol Ther. 2008; 16:1450–8. [PubMed: 18560419] Authours demonstrated the the effects of shape and size on cellular binding, internalization rates, and subcellular locallizations using CAM targeted nanoparticles.

[37•]. Torchilin VP. Multifunctional nanocarriers. Adv Drug Deliv Rev. 2006; 58:1532–55. [PubMed: 17092599] Thorough review which covers in detail the effects of nanoparticle type, surface

coating (with special attention paid to PEGylation), targeting moeities, charge and other design parameters on binding, uptake, subcellular localization, as it effects drug delivery over multiple pathologies.

[38]. Otsuka H, Nagasaki Y, Kataoka K. PEGylated nanoparticles for biological and pharmaceutical applications. Adv Drug Deliv Rev. 2003; 55:403–19. [PubMed: 12628324]

[39]. Fukukawa K, Rossin R, Hagooly A, Pressly ED, Hunt JN, Messmore BW, et al. Synthesis and characterization of core-shell star copolymers for in vivo PET imaging applications. Biomacromolecules. 2008; 9:1329–39. [PubMed: 18338840]

[40]. Anderson CJ, Bulte JW, Chen K, Chen X, Khaw BA, Shokeen M, et al. Design of targeted cardiovascular molecular imaging probes. J Nucl Med. 2010; 51(Suppl 1):3S–17S. [PubMed: 20395345]

[41]. Chen W, Jarzyna PA, van Tilborg GAF, Nguyen VA, Cormode DP, Klink A, et al. RGD peptide functionalized and reconstituted high-density lipoprotein nanoparticles as a versatile and multimodal tumor targeting molecular imaging probe. The FASEB Journal. 2010; 24:1689–99. [PubMed: 20075195]

[42]. Uppal R, Caravan P. Targeted Probes for Cardiovascular MR Imaging. Future Med Chem. 2010; 2:451–70. [PubMed: 20539821]

[43]. Nobs L, Buchegger F, Gurny R, Allemann E. Current methods for attaching targeting ligands to liposomes and nanoparticles. J Pharm Sci. 2004; 93:1980–92. [PubMed: 15236448]

[44]. Moghimi SM, Szebeni J. Stealth liposomes and long circulating nanoparticles: critical issues in pharmacokinetics, opsonization and protein-binding properties. Prog Lipid Res. 2003; 42:463–78. [PubMed: 14559067]

[45]. Torchilin VP. Recent advances with liposomes as pharmaceutical carriers. Nat Rev Drug Discov. 2005; 4:145–60. [PubMed: 15688077]

[46]. Buchanan KD, Huang S, Kim H, Macdonald RC, McPherson DD. Echogenic liposome compositions for increased retention of ultrasound reflectivity at physiologic temperature. J Pharm Sci. 2008; 97:2242–9. [PubMed: 17894368]

[47]. Hamilton AJ, Huang SL, Warnick D, Rabbat M, Kane B, Nagaraj A, et al. Intravascular ultrasound molecular imaging of atheroma components in vivo. J Am Coll Cardiol. 2004; 43:453–60. [PubMed: 15013130]

[48]. Kim H, Moody MR, Laing ST, Kee PH, Huang SL, Klegerman ME, et al. In vivo volumetric intravascular ultrasound visualization of early/inflammatory arterial atheroma using targeted echogenic immunoliposomes. Invest Radiol. 2010; 45:685–91. [PubMed: 20733507]

[49•]. Kamaly N, Miller AD. Paramagnetic liposome nanoparticles for cellular and tumour imaging. Int J Mol Sci. 2010; 11:1759–76. [PubMed: 20480040] Review describing bi-functional, bi-modal imaging paramagnetic liposome systems.

[50]. Li D, Patel AR, Klibanov AL, Kramer CM, Ruiz M, Kang BY, et al. Molecular Imaging of Atherosclerotic Plaques Targeted to Oxidized LDL Receptor LOX-1 by SPECT/CT and Magnetic Resonance. Circulation-Cardiovascular Imaging. 2010; 3:464–72. [PubMed: 20442371]

[51]. Marik J, Tartis MS, Zhang H, Fung JY, Kheirolomoom A, Sutcliffe JL, et al. Long-circulating liposomes radiolabeled with [^{18}F]fluorodipalmitin ([^{18}F]FDP). Nucl Med Biol. 2007; 34:165–71. [PubMed: 17307124]

[52]. Phillips WT, Goins BA, Bao A. Radioactive liposomes. Wiley Interdiscip Rev Nanomed Nanobiotechnol. 2009; 1:69–83. [PubMed: 20049780]

[53•]. Christian DA, Cai S, Bowen DM, Kim Y, Pajerowski JD, Discher DE. Polymersome carriers: from self-assembly to siRNA and protein therapeutics. Eur J Pharm Biopharm. 2009; 71:463–74. [PubMed: 18977437] Authors summarize the assembly and development of controlled release polymersomes to encapsulate therapeutics ranging from small molecule anti-cancer drugs to siRNA and therapeutic proteins.

[54]. Dziubla TD, Karim A, Muzykantov VR. Polymer nanocarriers protecting active enzyme cargo against proteolysis. J Control Release. 2005; 102:427–39. [PubMed: 15653162]

[55]. Laurent S, Forge D, Port M, Roch A, Robic C, Vander Elst L, et al. Magnetic iron oxide nanoparticles: synthesis, stabilization, vectorization, physicochemical characterizations, and biological applications. Chem Rev. 2008; 108:2064–110. [PubMed: 18543879]

[56]. Veiseh O, Gunn JW, Zhang M. Design and fabrication of magnetic nanoparticles for targeted drug delivery and imaging. Advanced Drug Delivery Reviews. 2010; 62:284–304. [PubMed: 19909778]

[57]. Weissleder R, Moore A, Mahmood U, Bhorade R, Benveniste H, Chiocca EA, et al. In vivo magnetic resonance imaging of transgene expression. Nat Med. 2000; 6:351–5. [PubMed: 10700241]

[58]. McCarthy JR, Weissleder R. Multifunctional magnetic nanoparticles for targeted imaging and therapy. Adv Drug Deliv Rev. 2008; 60:1241–51. [PubMed: 18508157]

[59]. Yallapu MM, Foy SP, Jain TK, Labhasetwar V. PEG-functionalized magnetic nanoparticles for drug delivery and magnetic resonance imaging applications. Pharm Res. 2010; 27:2283–95. [PubMed: 20845067]

[60]. Chorny M, Hood E, Levy RJ, Muzykantov VR. Endothelial delivery of antioxidant enzymes loaded into non-polymeric magnetic nanoparticles. J Control Release. 2010; 146:144–51. [PubMed: 20483366]

[61]. Hughes MS, Caruthers S, Tran TD, Marsh JN, Wallace K, Cyrus T, et al. Perfluorocarbon Nanoparticles for Molecular Imaging and Targeted Therapeutics. Proc IEEE. 2008; 96:397–415.

[62]. Soman NR, Lanza GM, Heuser JM, Schlesinger PH, Wickline SA. Synthesis and characterization of stable fluorocarbon nanostructures as drug delivery vehicles for cytolytic peptides. Nano Lett. 2008; 8:1131–6. [PubMed: 18302330]

[63]. Kaneda MM, Caruthers S, Lanza GM, Wickline SA. Perfluorocarbon nanoemulsions for quantitative molecular imaging and targeted therapeutics. Ann Biomed Eng. 2009; 37:1922–33. [PubMed: 19184435]

[64]. Lee CC, MacKay JA, Frechet JM, Szoka FC. Designing dendrimers for biological applications. Nat Biotechnol. 2005; 23:1517–26. [PubMed: 16333296]

[65]. Parrott MC, Benhabbour SR, Saab C, Lemon JA, Parker S, Valliant JF, et al. Synthesis, radiolabeling, and bio-imaging of high-generation polyester dendrimers. J Am Chem Soc. 2009; 131:2906–16. [PubMed: 19239268]

[66]. Jayagopal A, Russ PK, Haselton FR. Surface engineering of quantum dots for in vivo vascular imaging. Bioconjug Chem. 2007; 18:1424–33. [PubMed: 17760416]

[67]. Smith AM, Duan H, Rhyner MN, Ruan G, Nie S. A systematic examination of surface coatings on the optical and chemical properties of semiconductor quantum dots. Phys Chem Chem Phys. 2006; 8:3895–903. [PubMed: 19817050]

[68••]. Tsourkas A, Shinde-Patil VR, Kelly KA, Patel P, Wolley A, Allport JR, et al. In vivo imaging of activated endothelium using an anti-VCAM-1 magnetooptical probe. Bioconjug Chem. 2005; 16:576–81. [PubMed: 15898724] First description of anti-VCAM-1 Ab-targeted nanoparticles as proof-of-principles diagnotic imaging agents in inflammatory disease.

[69•]. Kelly KA, Allport JR, Tsourkas A, Shinde-Patil VR, Josephson L, Weissleder R. Detection of vascular adhesion molecule-1 expression using a novel multimodal nanoparticle. Circulation research. 2005; 96:327–36. [PubMed: 15653572] First description of peptide-targeted nanoparticles for diagnotic imaging of VCAM-1 expression in inflammation.

[70]. Nahrendorf M, Jaffer FA, Kelly KA, Sosnovik DE, Aikawa E, Libby P, et al. Noninvasive vascular cell adhesion molecule-1 imaging identifies inflammatory activation of cells in atherosclerosis. Circulation. 2006; 114:1504–11. [PubMed: 17000904]

[71]. McAteer MA, Sibson NR, von Zur Muhlen C, Schneider JE, Lowe AS, Warrick N, et al. In vivo magnetic resonance imaging of acute brain inflammation using microparticles of iron oxide. Nat Med. 2007; 13:1253–8. [PubMed: 17891147]

[72•]. Hoyte LC, Brooks KJ, Nagel S, Akhtar A, Chen R, Mardiguian S, et al. Molecular magnetic resonance imaging of acute vascular cell adhesion molecule-1 expression in a mouse model of cerebral ischemia. J Cereb Blood Flow Metab. 2010; 30:1178–87. [PubMed: 20087364] This paper outlines the first use of VCAM-1 targeted MPIO for imaging cerebral ischemia *in vivo*.

[73]. Southworth R, Kaneda M, Chen J, Zhang L, Zhang H, Yang X, et al. Renal vascular inflammation induced by Western diet in ApoE-null mice quantified by ^{19}F NMR of VCAM-1 targeted nanobeacons. Nanomedicine. 2009; 5:359–67. [PubMed: 19523428]

[74]. Kaufmann BA, Carr CL, Belcik JT, Xie A, Yue Q, Chadderdon S, et al. Molecular imaging of the initial inflammatory response in atherosclerosis: implications for early detection of disease. Arterioscler Thromb Vasc Biol. 2010; 30:54–9. [PubMed: 19834105]

[75•]. Rossin R, Muro S, Welch MJ, Muzykantov VR, Schuster DP. In vivo imaging of ^{64}Cu-labeled polymer nanoparticles targeted to the lung endothelium. J Nucl Med. 2008; 49:103–11. [PubMed: 18077519] Small-animal PET imaging used to track ICAM-1 targeted, ^{64}Cu nanoparticles in vivo. Nanoparticles were able to detect pulmonary endothelium inflammation within 45 min of inflammatory insult. Signal persisted up to 24 h p.i.

[76]. Danilov SM, Gavrilyuk VD, Franke FE, Pauls K, Harshaw DW, McDonald TD, et al. Lung uptake of antibodies to endothelial antigens: key determinants of vascular immunotargeting. American journal of physiology. 2001; 280:L1335–47. [PubMed: 11350815]

[77]. Muro S, Dziubla T, Qiu W, Leferovich J, Cui X, Berk E, et al. Endothelial targeting of high-affinity multivalent polymer nanocarriers directed to intercellular adhesion molecule 1. J Pharmacol Exp Ther. 2006; 317:1161–9. [PubMed: 16505161]

[78]. Reynolds PR, Larkman DJ, Haskard DO, Hajnal JV, Kennea NL, George AJ, et al. Detection of vascular expression of E-selectin in vivo with MR imaging. Radiology. 2006; 241:469–76. [PubMed: 17005768]

[79]. Chapon C, Franconi F, Lacoeuille F, Hindre F, Saulnier P, Benoit JP, et al. Imaging E-selectin expression following traumatic brain injury in the rat using a targeted USPIO contrast agent. MAGMA. 2009; 22:167–74. [PubMed: 19107536]

[80•]. van Kasteren SI, Campbell SJ, Serres S, Anthony DC, Sibson NR, Davis BG. Glyconanoparticles allow pre-symptomatic in vivo imaging of brain disease. Proc Natl Acad Sci U S A. 2009; 106:18–23. [PubMed: 19106304] Carbohydrate-functionalized nanoparticles were directed to endothelial markers E- and P-selectin in acute inflammation. Nanoparticles allowed pre-symptomatic MRI imaging of acute inflammation within the brain.

[81]. Jin AY, Tuor UI, Rushforth D, Filfil R, Kaur J, Ni F, et al. Magnetic resonance molecular imaging of post-stroke neuroinflammation with a P-selectin targeted iron oxide nanoparticle. Contrast Media Mol Imaging. 2009; 4:305–11. [PubMed: 19941323]

[82]. Buttgereit F, Burmester GR, Lipworth BJ. Optimised glucocorticoid therapy: the sharpening of an old spear. Lancet. 2005; 365:801–3. [PubMed: 15733723]

[83]. Muzykantov VR. Biomedical aspects of targeted delivery of drugs to pulmonary endothelium. Expert Opin Drug Deliv. 2005; 2:909–26. [PubMed: 16296786]

[84]. Carnemolla R, Shuvaev VV, Muzykantov VR. Targeting antioxidant and antithrombotic biotherapeutics to endothelium. Semin Thromb Hemost. 2010; 36:332–42. [PubMed: 20490983]

[85•]. Homem de Bittencourt PI Jr. Lagranha DJ, Maslinkiewicz A, Senna SM, Tavares AM, Baldissera LP, et al. LipoCardium: endothelium-directed cyclopentenone prostaglandin-based liposome formulation that completely reverses atherosclerotic lesions. Atherosclerosis. 2007; 193:245–58. [PubMed: 16996518] VCAM-1 targeted liposomes delivering an anti-inflammatory therapeutic were used in an atherosclerosis mouse model. Targeted liposomes used to treat mice resulted in the complete recovery of vascular injuries, while untreated died within 2 weeks.

[86]. Garnacho C, Dhami R, Simone E, Dziubla T, Leferovich J, Schuchman EH, et al. Delivery of acid sphingomyelinase in normal and niemann-pick disease mice using intercellular adhesion molecule-1-targeted polymer nanocarriers. J Pharmacol Exp Ther. 2008; 325:400–8. [PubMed: 18287213]

[87]. Muro S, Gajewski C, Koval M, Muzykantov VR. ICAM-1 recycling in endothelial cells: a novel pathway for sustained intracellular delivery and prolonged effects of drugs. Blood. 2005; 105:650–8. [PubMed: 15367437]

[88]. Calderon AJ, Bhowmick T, Leferovich J, Burman B, Pichette B, Muzykantov V, et al. Optimizing endothelial targeting by modulating the antibody density and particle concentration of anti-ICAM coated carriers. J Control Release. 2010

[89•]. Herbst SM, Klegerman ME, Kim H, Qi J, Shelat H, Wassler M, et al. Delivery of Stem Cells to Porcine Arterial Wall with Echogenic Liposomes Conjugated to Antibodies against CD34 and Intercellular Adhesion Molecule-1. Mol Pharm. 2009; 7:3–11. [PubMed: 19719324] The authors describe the use of ICAM-1 targeted liposomes to deliver therapeutic stem cells to the site of vascular injury associated with atherosclerosis. These particles are echogenic and ultrasound treatment during delivery resulted in a greater accumulation of stem cells at the site of vascular injury.

[90•]. Asgeirsdottir SA, Zwiers PJ, Morselt HW, Moorlag HE, Bakker HI, Heeringa P, et al. Inhibition of proinflammatory genes in anti-GBM glomerulonephritis by targeted dexamethasone-loaded AbEsel liposomes. Am J Physiol Renal Physiol. 2008; 294:F554–61. [PubMed: 18160627] This work outlines the use of E-selectin targeted liposomes for delivery of dexamethasone to treat vascular inflammation in the kidneys. Mice given the targeted therapeutic have reduced kidney inflammation by nearly 70% and untargeted effects of dexamethasone are kept to a minimum.

[91]. Hashida N, Ohguro N, Yamazaki N, Arakawa Y, Oiki E, Mashimo H, et al. High-efficacy site-directed drug delivery system using sialyl-Lewis X conjugated liposome. Exp Eye Res. 2008; 86:138–49. [PubMed: 18036523]

[92]. Ferrante EA, Pickard JE, Rychak J, Klibanov A, Ley K. Dual targeting improves microbubble contrast agent adhesion to VCAM-1 and P-selectin under flow. J Control Release. 2009; 140:100–7. [PubMed: 19666063]

[93]. Weller GE, Villanueva FS, Tom EM, Wagner WR. Targeted ultrasound contrast agents: in vitro assessment of endothelial dysfunction and multi-targeting to ICAM-1 and sialyl Lewisx. Biotechnol Bioeng. 2005; 92:780–8. [PubMed: 16121392]

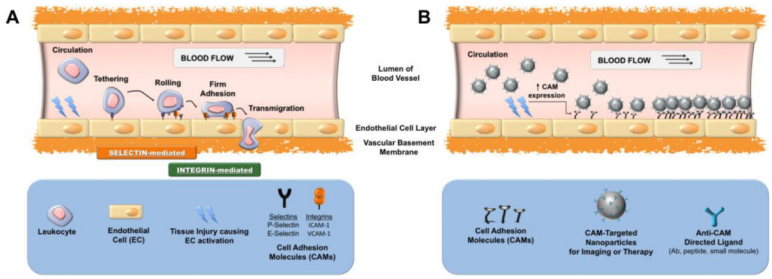

Figure 1.

Cell adhesion molecule (CAM)-mediated approach to the delivery of diagnostic and/or therapeutic nanoparticles to injured vascular endothelium in early inflammation. (A) Leukocyte adhesion and transmigration mediated by CAMs resulting in propagation of inflammation; (B) Imaging or therapy of vascular sites of early inflammation via delivery of CAM-targeted nanoparticles.

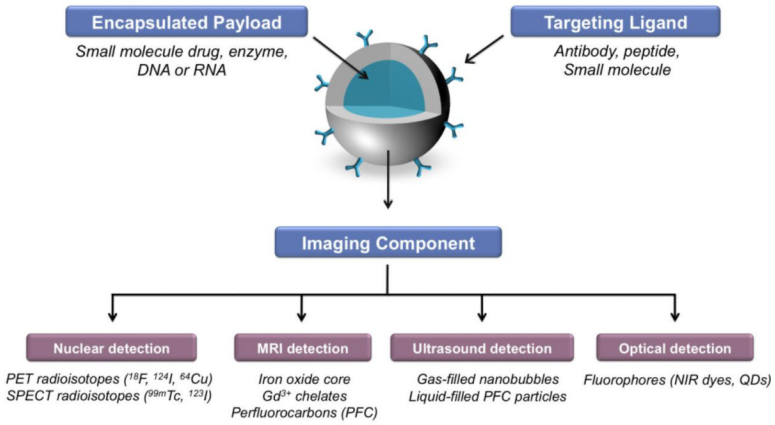

Figure 2.

Schematic representation of targeted nanoparticles engineered for biomedical imaging and therapeutic drug delivery applications. The components of a multifunctional nanocarrier can include a ligand for cellular targeting, and an encapsulated payload for delivery of the therapeutic agents. The imaging components (e.g. radioisotope, NIR dye) can be incorporated in the interior payload, on the targeting ligand or associated with the nanoparticle shell, for example.

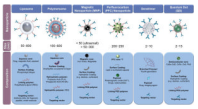

Figure 3.
Classes of nanoparticles for imaging and drug delivery, including their size and composition.

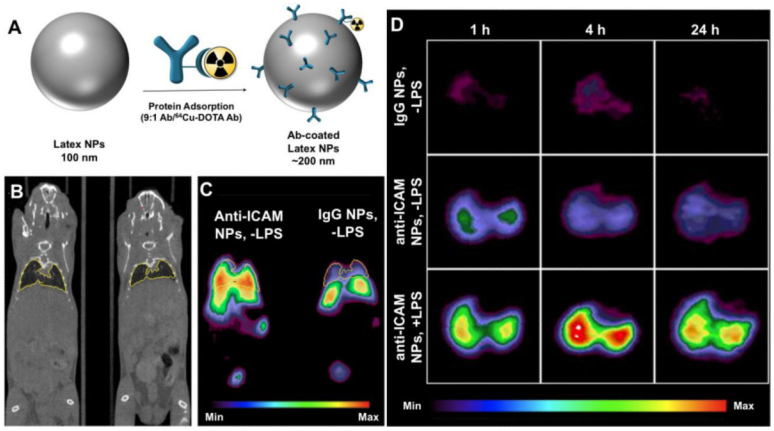

Figure 4.

(A) Preparation of 200 nm Ab-coated polymeric latex NPs for ^{64}Cu PET imaging. ^{64}Cu was chelated to 1,4,7,10-tetraazacyclododecane-1,4,7,10-tetraacetic acid (DOTA) preconjugated to IgG, and then mixed with unlabeled anti-ICAM or IgG Ab (1:9) for adsorption onto NP surface (~250 Ab/NP). (B) MicroCT (coronal slice) and (C) microPET (coronal slice) images of 2 naïve mice (−LPS) injected with ICAM-targeted NPs or control IgG-coated NPs 1 h p.i. (D) Representative decay-corrected transverse micro-PET images of naïve mice (−LPS) and LPS-challenged mice (+LPS) at 1, 4, and 24 h after NP administration. Uptake intensity map is normalized to the highest pixels in the LPS-challenged mice. Figure modified from [75]. © 2008 Society of Nuclear Medicine.

Curr Opin Colloid Interface Sci. Author manuscript; available in PMC 2012 June 1.

Table 1

[a] Endothelial cell adhesion molecules (CAMs) as early markers of vascular inflammation.

Superfamily	**Lectin Adhesion Molecules**		**Ig-superfamily Cell Adhesion Molecules**		
Cell Adhesion Molecule (CAM)	**P-Selectin[b,c]**	**E-Selectin**	**VCAM-1**	**ICAM-1**	**PECAM-1**
CD Classification	CD62P	CD62E	CD106	CD54	CD31
Surface Expression	Inducible	Inducible	Inducible	Constitutive and up-regulated upon induction	Constitutive
Temporal Expression	Expression is fast and transient; internalized within 20 min	Peak expression at 4 h (*in vitro*); declines to baseline within 24 h during inflammation	Very low copies/cell; increases to 10^4–10^5 copies/cell	10^4–10^5 copies/cell in normal tissue[d]; 3 to 5-fold increase in inflammation	10^6 copies/cell
Ligands	Leukocyte expressing sialyl-Lewis X	Leukocyte expressing sialyl-Lewis X	Leukocyte with β1 integrin VLA-4 (α4β1) and α4β7	Leukocyte with β2 integrins (e.g. LFA-1 and Mac-1)	Leukocyte with β1 & β3 integrins Heparin proteoglycans
Function	Leukocyte tethering and rolling		Leukocyte firm adhesion		Leukocytes transmigration; Angiogenesis

[a] Modified from Muro and Muzykantov [4];

[b] P-Selectin is present in granules within endothelial cells; upon inflammation it is transported to apical cell membrane; Induced expression of E-selectin, VCAM-1 and ICAM-1 is due to *de novo* protein synthesis ;

[c] P-selectin is also expressed on platelets;

[d] [6].

Table 2

Sensitivity and resolution of *in vivo* molecular imaging modalities available for monitoring endothelial-targeted nanoparticles.

Imaging modality	Radiation Spectrum	Contrast Agents	Sensitivity	Spatial Resolution	Advantages	Disadvantages
PET	High energy gamma rays	Positron Emitters ^{18}F, ^{124}I, ^{64}Cu	10^{-11}–10^{-12}M	1–2 mm	High sensitivity	Low resolution Requires cyclotron produced isotopes
SPECT	Low energy gamma rays	Photon Emitters ^{123}I, ^{99m}Tc, ^{111} In	10^{-10}–10^{-11}M	1–2 mm	High sensitivity	Low resolution
MRI	Radiowaves	Gadolinium (Gd^{3+}) chelates, iron oxide	10^{-3}–10^{-5}M[a]	25–200 μm	High resolution	Low sensitivity; long image acquisition time and processing time
Ultrasound (US)	High-frequency sound	Gas-filled bubbles	10^{-6}–10^{-9}M[b]	30–500 μm[b]	Low cost; realtime imaging; portability	Limited resolution[c]; Difficulty imaging through bone and lungs
Optical Fluorescence	Visible or near-infrared light	Fluorophores	10^{-9}–10^{-12}M	1–10 mm	High sensitivity; low cost; high throughput	Low resolution; Limited depth to less than 1 cm

[a] With contrast-loaded nanoparticles the sensitivity can be enhanced to 10^{-9}M.

[b] [16]

[c] The spatial resolution of US indicated is at the surface of the body. The sensitivity and resolution decreases as a function of depth of penetration of the acoustic signal.